Integrative and Comparative Biology

Integrative and Comparative Biology, volume 59, number 2, pp. 394–409
doi:10.1093/icb/icz022

Society for Integrative and Comparative Biology

SYMPOSIUM

Functional coupling in the evolution of suction feeding and gill ventilation of sculpins (Perciformes: Cottoidei)

S. C. Farina,[1,*] M. L. Knope,[†] K. A. Corn,[‡] A. P. Summers[§] and W. E. Bemis[¶]

*Department of Biology, Howard University, 415 College Street NW, Washington, DC 20059, USA; [†]Department of Biology, University of Hawaii, Hilo, 200 West Kawili Street, Hilo, HI 96720, USA; [‡]Department of Evolution and Ecology, University of California Davis, 1 Shields Avenue, Davis, CA 95616, USA; [§]Friday Harbor Laboratories, University of Washington, Friday Harbor, WA 98250, USA; [¶]Department of Ecology and Evolutionary Biology, Cornell University, 215 Tower Road, Ithaca, NY 14853, USA

From the symposium "Multifunctional structures and multistructural functions: Functional coupling and integration in the evolution of biomechanical systems" presented at the annual meeting of the Society for Integrative and Comparative Biology, January 3–7, 2019 at Tampa, Florida.

[1]E-mail: stacy.farina@howard.edu

Synopsis Suction feeding and gill ventilation in teleosts are functionally coupled, meaning that there is an overlap in the structures involved with both functions. Functional coupling is one type of morphological integration, a term that broadly refers to any covariation, correlation, or coordination among structures. Suction feeding and gill ventilation exhibit other types of morphological integration, including functional coordination (a tendency of structures to work together to perform a function) and evolutionary integration (a tendency of structures to covary in size or shape across evolutionary history). Functional coupling, functional coordination, and evolutionary integration have each been proposed to limit morphological diversification to some extent. Yet teleosts show extraordinary cranial diversity, suggesting that there are mechanisms within some teleost clades that promote morphological diversification, even within the highly integrated suction feeding and gill ventilatory systems. To investigate this, we quantified evolutionary integration among four mechanical units associated with suction feeding and gill ventilation in a diverse clade of benthic, primarily suction-feeding fishes (Cottoidei; sculpins and relatives). We reconstructed cottoid phylogeny using molecular data from 108 species, and obtained 24 linear measurements of four mechanical units (jaws, hyoid, opercular bones, and branchiostegal rays) from micro-CT reconstructions of 44 cottoids and 1 outgroup taxon. We tested for evolutionary correlation and covariation among the four mechanical units using phylogenetically corrected principal component analysis to reduce the dimensionality of measurements for each unit, followed by correlating phylogenetically independent contrasts and computing phylogenetic generalized least squares models from the first principle component axis of each of the four mechanical units. The jaws, opercular bones, and branchiostegal rays show evolutionary integration, but the hyoid is not positively integrated with these units. To examine these results in an ecomorphological context, we used published ecological data in phylogenetic ANOVA models to demonstrate that the jaw is larger in fishes that eat elusive or grasping prey (e.g., prey that can easily escape or cling to the substrate) and that the hyoid is smaller in intertidal and hypoxia-tolerant sculpins. Within Cottoidei, the relatively independent evolution of the hyoid likely has reduced limitations on morphological evolution within the highly morphologically integrated suction feeding and gill ventilatory systems.

Introduction

To understand the evolution of complex functional anatomical systems, we must consider how evolutionary forces act on a system at all levels of functional complexity. Studies of functional evolutionary morphology typically examine the evolution of structures in the context of performance of a specific function. However, although some structures appear to have evolved for a singular purpose, such as the baleen of whales or the suction disc of remoras, most structures perform many functions. This reflects a fundamental reality of whole organisms—most

Advance Access publication April 20, 2019

ubiquitous behaviors (e.g., eating, breathing, and locomotion) require coordination of many structures of the head and body (Wainwright 2007; Walker 2010). The overlap of structures among multiple functions is known as *functional coupling*. The few existing studies that address macroevolution of structures that perform multiple functions have centered around the idea that functional coupling limits morphological evolution. For example, rates of cranial morphological evolution were shown to be much lower in cichlids that use mouth brooding as opposed to other types of parental care (Tsuboi et al. 2015). Presumably, this is because the additional function of brooding constrains the morphology of the buccal cavity, which also must be used for eating and breathing (Hoey et al. 2012; Tsuboi et al. 2015). Additionally, a classic example of evolutionary innovation in fishes is the evolution of specialized pharyngeal jaws in cichlids and wrasses (Liem 1973; Kaufman and Liem 1982; Wainwright 2006). Many teleost fishes use their oral jaws for both prey capture and prey processing (e.g., manipulation and mechanical breakdown), but many also have specialized pharyngeal jaws used for prey processing (Wainwright 2006). In cichlids (Cichlidae) and wrasses (Labridae), such functional decoupling of prey capture and processing is considered a key innovation that has contributed to morphological diversity within these clades (Liem 1973; Wainwright 2006). Although these examples are compelling, there are counter-examples in which functional coupling is associated with increased diversity. The most striking example is the elytra of beetles (Coleoptera). Beetles exhibit extraordinary morphological diversity and species richness (Lawrence et al. 2011), and yet their key innovation, modified forewings (elytra), are a prime example of functional coupling, because they are used in both protection and flight (Dudley 2002; Johansson et al. 2012). Such functional coupling does not seem to have limited morphological diversification of beetles. Similarly, teleost fishes are the most diverse clade of vertebrates with more than 33,000 extant species (Eschmeyer and Fong 2019), and they have two major innovations: powerful suction feeding and an efficient double-pump system of gill ventilation. These two systems are highly functionally coupled, with both using many of the same structures, and yet this does not appear to have limited morphological or species diversity within teleosts.

Morphological integration can occur across many levels of biological organization and is central to the discussion of functional anatomical evolution. The term *morphological integration* refers to any functional coordination or evolutionary covariation among structures (Olson and Miller 1958; Cheverud 1996; Klingenberg 2008). This definition is intentionally broad (Cheverud 1996; Klingenberg 2008), because it encompasses the many areas of study necessary to develop a holistic understanding of integration, including fields as disparate as quantitative genetics, functional morphology, biomechanics, developmental biology, and paleontology. However, such a generalized definition makes it difficult to standardize terminology for the study of morphological evolution across a broad range of disciplines. Here, we use a functional anatomical framework to discuss these terms and concepts, and we demonstrate how they can be holistically applied to a specific example – cranial evolution in teleost fishes. For the study of the evolution of complex anatomical systems, we recognize four levels of morphological integration (Table 1). We use *phenotypic integration* to refer to any correlation or covariation of size or shape of structures within an individual or population. The term "phenotypic" is meant to reflect the convention that a phenotype is defined at the level of the individual. *Functional coordination* concerns multiple structures that work together to perform a specific function. *Functional coupling*, as defined previously, comes into play when a structure is involved with the performance of more than one function. At the interspecies level is *evolutionary integration*, which refers to correlation and co-variation among structures across taxa and evolutionary history.

Table 1 Types of morphological integration

Term	Definition
Morphological integration	Any coordination, covariation, or correlation among structures (Cheverud 1996; Klingenberg 2008)
Phenotypic integration	Correlation or covariation in size or shape of structures within an individual or population (Parsons et al. 2011)
Functional coordination	Multiple structures working together to perform a single function with a high degree of biomechanical coordination (Schwenk and Wagner 2001; Collar et al. 2014)
Functional coupling	Overlap in structures used to perform two or more separate functions (Wainwright 2007; Tsuboi et al. 2015)
Evolutionary integration	Correlation or covariation in size or shape of structures across evolutionary history (Olson and Miller 1958; Cheverud 1996; Monteiro and Nogueira 2010; Claverie and Patek 2013)

We define types of morphological integration in an evolutionary and functional context.

All levels of morphological integration have the potential to influence the evolution of musculoskeletal structures through complex interactions. These interactions are primarily discussed through the lens of morphological diversity (disparity), with most types of integration historically considered to constrain the extent of morphological evolution by either limiting the morphospace that a structural system can occupy or by reducing the rate of morphological change (Felice et al. 2018). For example, functional coordination has been thought to constrain morphological evolution, because structures that must move in a coordinated manner may be shaped by similar evolutionary influences for performance of a function (Schwenk and Wagner 2001; Collar et al. 2014; Roberts et al. 2018). As mentioned, functional coupling has been shown to constrain morphological evolution (Hoey et al. 2012; Tsuboi et al. 2015), because sets of structures performing multiple functions are limited by mechanical and physiological constraints of all of the functions performed (Lauder 1981; Schaefer and Lauder 1996; Walker 2010). Phenotypic and evolutionary integration are products of complex interactions among genes, developmental processes, performance (including functional coordination and multifunctionality), and evolutionary forces acting on them (Cheverud 1982; Hulsey et al. 2005; Young and Hallgrímsson 2005; Klingenberg 2008; Goswami and Polly 2010; Parsons et al. 2011, 2018). Therefore, there is not always a clear relationship between evolutionary integration and functions of structures (Goswami 2006; Claverie and Patek 2013; Klingenberg and Marugán-Lobón 2013). However, a high degree of evolutionary integration can indicate that a system is constrained by covariation that limits evolutionary variability of morphology within clades (Collar et al. 2014). A lack of evolutionary covariation among structures or parts of structures is termed *evolutionary modularity*, and the tendency for structures or modules to evolve independently within a functional system can be considered a source of relaxed constraint on morphological disparity in some systems (Goswami and Polly 2010; Parnell et al. 2012; Claverie and Patek 2013; Goswami et al. 2014).

To unite the concepts of evolutionary integration with functional coordination and coupling, we group structures into mechanical units (=*functional modules*; Breuker et al. 2006; Klingenberg 2008; Córdoba and Cocucci 2011) based on their mechanical connections and their tendency to move together in a mechanically coordinated manner. Mechanical units may show internal phenotypic or evolutionary integration, but this is not necessary to recognize or define them (Breuker et al. 2006; Klingenberg 2008), which is why we avoid the term *module*. Here, we define four mechanical units: (1) jaws, (2) hyoid, (3) opercular bones, and (4) branchiostegals. The jaws, hyoid, and opercular bones are essential for two functionally coupled systems of teleosts: suction feeding and gill ventilation (Lauder 1980, 1983). Suction feeding is the ancestral feeding strategy for jawed vertebrates (Wainwright et al. 2015), and its ubiquity among actinopterygians (Lauder 1982) and early-branching sarcopterygians (e.g., coelacanths, Lauder 1980; lungfishes, Bemis and Lauder 1986; Bemis 1987a) makes it critical to studies of vertebrate evolution. Suction feeding involves rapid expansion of the buccal chamber, creating negative pressures that draw water and prey into the mouth. Powerful suction feeding with jaw protrusion is considered to be a key innovation that lead, in part, to morphological diversity and species richness of teleosts (Wainwright et al. 2015; Wainwright and Longo 2017). Rapid buccal expansion requires movements of the jaws, hyoid, and opercular bones. The expansive phase of suction feeding begins with an increase in gape (Lauder 1985), accomplished by depression of the lower jaw (dentary and anguloarticular, *dn* and *an* in Fig. 1) caused by posterodorsal rotation of the opercular bones (opercle, subopercle, and interopercle, *op*, *so*, and *io* in Fig. 1; Liem 1970; Anker 1974; Lauder 1982). Subsequently, protrusion of the upper jaw (*pm* and *mx* in Fig. 1), lateral expansion of the suspensorium, and ventral depression of the hyoid (*cha* and *chp* in Fig. 1) expand the volume of the oral cavity and further depress the lower jaw. Dorsal rotation of the neurocranium and retraction of the pectoral girdle by epaxial and hypaxial muscles, respectively, also contribute to buccal expansion (Lauder 1985; Camp and Brainerd 2014, 2015). Pump gill ventilation is the most common form of gill ventilation among teleosts, with other strategies including ram ventilation (swimming with an opened mouth to force water over the gills) and aerial ventilation (Brainerd and Ferry-Graham 2006). Pump ventilation relies on changes in water pressure driven by structures of the buccal and gill chambers. These chambers act as pumps, expanding and compressing cyclically to produce unidirectional water flow over the gills (Hughes and Shelton 1958; Hughes 1960). Movements of the buccal and gill chambers coordinate with one another, but the chambers perform different tasks to move water over the gills. The buccal pump generates negative pressure to draw water into the mouth during inhalation, followed by

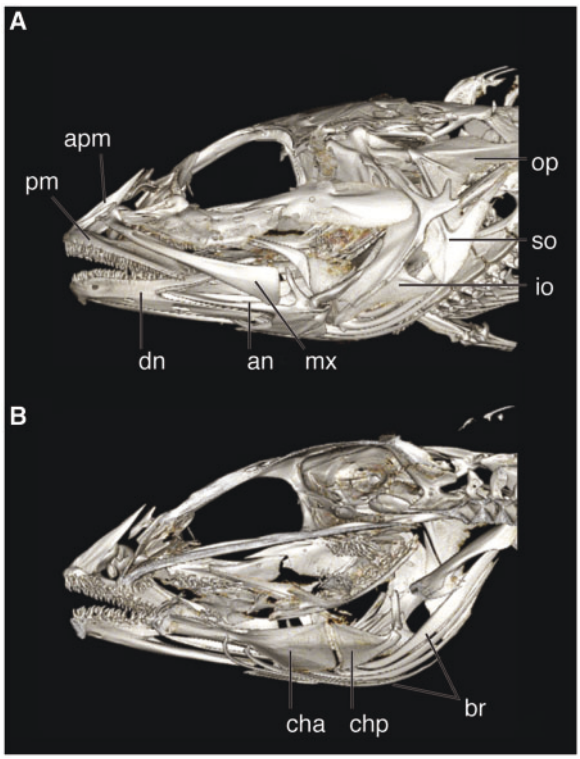

Fig. 1 Skeletal anatomy of the cottoid skull. Micro-CT reconstruction of *Artedius lateralis* showing morphological components of the jaws, hyoid apparatus, opercular bones, and branchiostegals from an external view (**A**) and in a sagittal section (**B**). Apm, ascending process of the premaxilla; an, anguloarticular; br, branchiostegals; cha, anterior ceratohyal; chp, posterior ceratohyal; dn, dentary; io, interopercle; mx, maxilla; op, opercle; pm, premaxilla; so, subopercle.

positive pressure to force water from the mouth over the gills. The gill chamber pump generates negative pressure to draw water over the gills and into the gill chamber, followed by positive pressure to force water out of the gill opening during exhalation. The buccal pump primarily includes the jaws and hyoid, whereas the gill chamber pump consists of the opercular bones and the fourth mechanical unit, the branchiostegal rays (*br* in Fig. 1).

In addition to their functional coupling, suction feeding and gill ventilation in teleosts show evidence of high functional coordination and evolutionary integration among the structures involved (Sanford and Wainwright 2002; Gibb and Ferry-Graham 2005; Collar et al. 2014; Kane and Higham 2015). Given the aforementioned associations of functional coupling, functional coordination, and evolutionary integration with constraint on morphological evolution, it is perhaps surprising that there is so much diversity in cranial morphology among teleosts. However, we predict that many teleost clades have sources of relaxed morphological constraint within these complex systems, which allows morphological diversification to occur. We examined this possibility in Cottoidei (*sensu* Smith and Busby 2014), which includes sculpins, poachers, snailfishes, lumpsuckers, and sandfishes and about 859 valid species to date (Eschmeyer and Fong 2019) in 13 families (Smith and Busby 2014; van der Laan et al. 2014). Cottoids are ecologically diverse, ranging from intertidal to deep sea habitats, from sit-and-wait predators to active hunters, and from small to large sizes at maturity (Knope and Scales 2013; Buser et al. 2017). However, almost all cottoids are demersal suction feeders and pump gill ventilators, with variation in prey choice and feeding performance (Norton 1995; Napazakov and Chuchukalo 2005; Thedinga et al. 2006; Glubokov and Orlov 2008). Cottoidei has been the subject of extensive phylogenetic study and revision (Smith and Wheeler 2004; Ramon and Knope 2008; Knope 2013; Smith and Busby 2014; Buser and López 2015). Here, we use available molecular data to reconstruct cottoid phylogeny and test four hypotheses of evolutionary integration among the four mechanical units defined above (Fig. 2). Our first hypothesis (H1; Fig. 2A) is that the three mechanical units associated with rapid expansion of the buccal cavity during suction feeding will show significant evolutionary integration, based on their high functional coordination. Our second hypothesis (H2; Fig. 2B) is that mechanical units of the buccal and gill chambers will show significant within-chamber evolutionary integration but lack between-chamber integration, based on the tight within-chamber functional coordination during ventilatory pumping (Fig. 2B). Our third hypothesis (H3; Fig. 2C) is that the pattern of evolutionary integration among these units will reflect development, with the dermal skeleton of the jaws, opercular bones, and branchiostegal rays showing significant evolutionary integration, based on their similar developmental origins as dermal bones (except for the articular part of the anguloarticular) relative to the endochondral origin of the hyoid (de Beer 1937; Hall 2015). Our last hypothesis (H4; Fig. 2D) is that all mechanical units will show significant evolutionary integration based on the high degree of functional coupling between suction feeding and gill ventilation (Liem 1970; Lauder 1980, 1983). To relate our morphological measurements to ecology, we use data from studies of sculpin diet (Norton 1995), habitat (Eschmeyer et al. 1983), and hypoxia tolerance (Mandic et al. 2009, 2013) to test associations among ecological variables and mechanical units within a subset of cottoids examined.

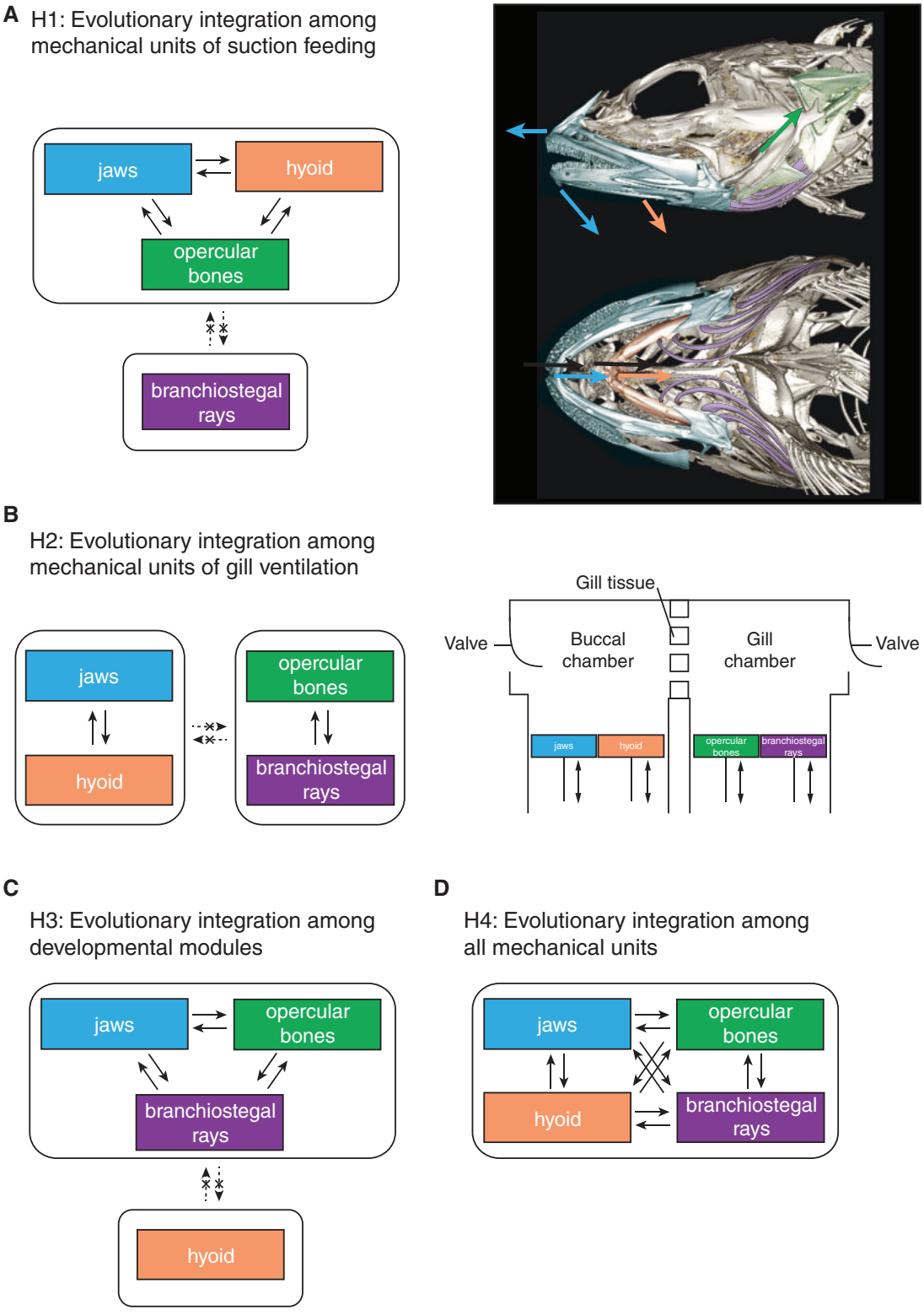

Fig. 2 Four hypotheses of evolutionary integration among mechanical units of the skull. (**A**) H1: Mechanical units associated with suction feeding (jaws, hyoid, and opercular bones) will show significant evolutionary integration, based on functional coordination necessary for rapid buccal expansion, during which the upper jaw protrudes (blue) and the lower jaw (blue) is depressed by dorsal opercular rotation (green) and hyoid retraction (orange). (**B**) H2: Mechanical units of buccal and gill chambers will show significant within-chamber evolutionary integration but lack between-chamber integration, based on within-chamber functional integration during ventilatory pumping. (**C**) H3: The jaws, opercular bones, and branchiostegal rays will show significant evolutionary integration, based on their similar developmental origins relative to the hyoid. (**D**) H4: All mechanical units will show significant evolutionary integration, based on the high degree of functional coupling between suction feeding and gill ventilation.

Materials and methods

Phylogenetic reconstruction

We reconstructed a phylogeny of Cottoidei using mitochondrial and nuclear gene sequence data for 106 species of cottoids and two outgroup species, *Hexagrammos decagrammus* and *H. stelleri* (Online Appendix Table SA1). We used a molecular dataset from Knope (2013), which included sequences from mitochondrial gene cytochrome b (*cytb*) and the first nuclear intron of the S7 ribosomal protein (*S7*) for 99 cottoid species. We supplemented these data with sequences from GenBank (Benson et al. 2013), including *cytb* from seven additional species of cottoids and the two outgroup species as well as *S7* for the two outgroup species. We also included GenBank sequences from mitochondrial gene cytochrome c oxidase I (*COI*) for a subset of 72 taxa. Sequences from each gene were aligned individually using MUSCLE (Edgar 2004) on the EMBL–EBI bioinformatics web tool (Li et al. 2015). The complete alignment had 86.7% amplicon and 69.3% base pair coverage. Best-fit nucleotide substitution models were chosen using jModelTest v2.1.7 (Guindon and Gascuel 2003; Darriba et al. 2012) based on AIC values calculated for 24 candidate models.

We constructed trees using *MrBayes* v3.2.3 (Ronquist et al. 2012) on the CIPRES Science Gateway v3.3. We computed 36 *MrBayes* runs with seven gene partitions and an MCMC chain length of 20,000,000. Nucleotide substitution models were chosen for our seven partitions based on jModelTest results. We used a general time-reversible model (Tavaré 1986) with invariable sites and rate variation among sites (GTR + I + G) for *S7* and *cytb* (codon positions 1, 2, and 3). For the *COI* gene, we used a general time-reversible model with equal state frequencies (SYM) for codon position 1, the F81 model (Felsenstein 1981) for codon position 2, and a general time-reversible model with rate variation among sites (GTR + G) for codon position 3. Each of the 36 *MrBayes* runs were evaluated for quality in *Tracer* v1.6.0 (Rambaut et al. 2014), and the 20 runs with the highest effective sample size for the mean likelihood score were used to construct 20 maximum clade credibility (MCC) trees in *Tree Annotator* v1.8.0. We determined which tree topologies best explained our molecular data with a Shimodaira–Hasegawa test using the *SH.test* function in the *phangorn* R package (Shimodaira and Hasegawa 1999; Schliep 2011; R Core Team 2016), and the results are listed in Online Appendix Table SA2.

Morphological measurements

We measured cranial skeletal elements from 44 cottoids and one outgroup taxon (*Hexagrammos stelleri*) ranging in head length from 6 to 35 mm. We collected and measured 17 species from marine habitats near Friday Harbor Laboratories on San Juan Island, Washington (Cornell University IACUC 2013-0017) and accessioned them into the Cornell University Museum of Vertebrates (Online Appendix Table SB1). Individuals were identified to species using Eschmeyer et al. (1983). We supplemented these with measurements from specimens already in the collection (*Rhamphocottus richardsonii* [CU54050], *Xeneretmus latifrons* [CU71854], and *Cottus cognatus* [CU78131]). We imaged the specimens using micro-computed tomography (micro-CT) at the Cornell University Biotechnology Resource Center's Imaging Facility (GE eXplore CT-120 or an Xradia Versa XRM-520). Each fish was scanned from the pectoral girdle to the anterior-most point of the head. Voxel size ranged from 14 to 50 μm^3, with smaller specimens scanned at lower voxel sizes. DICOM files are available for public download on Morphosource.org. We further supplemented our dataset with 25 cottoid scans downloaded from Morphosource.org (Online Appendix Table SB1). We imported DICOM or JPG files from each scan into OsiriX (version 6.0.2 64-bit; Rosset et al. 2004) or Horos software (Nimble Co LLC, Annapolis, MD, USA) and used the "3D multiplanar reconstruction" tool to view the 3D reconstruction simultaneously in three orthogonal planes. To obtain linear measurements from each structure, we began with the specimen oriented such that we could view the sagittal, transverse, and frontal planes. We then rotated the planes until the entire length of the structure was in view in one plane by overlaying the axes of the other two planes (using the "Axis" tool) in the measurement plane, in which we measured the dimensions of the structure.

We collected linear measurements in this manner from the four previously noted mechanical units of the head: jaws, hyoid, opercular bones, and branchiostegals. Jaw measurements were: length of the maxilla, maximum height of the maxilla, length of the premaxilla, length of the ascending process of the premaxilla, lengths of the dentary from the anterior tip to the posterior tip of the dorsal and ventral processes, length of the anguloarticular from the anterior tip to the jaw joint, height of the anguloarticular at the jaw joint, and distance between the left and right jaw joints. Hyoid measurements were: length and height of the anterior ceratohyal, length

and height of the posterior ceratohyal (=epihyal of some authors; see Grande and Bemis 1998: 23), and length of the urohyal. Opercular bone measurements were: length of the opercle from the joint with the hyomandibula to the posterior tip of the opercle and length of the opercle from the joint to the posterior margin of the opercle (horizontal from the joint with the hyomandibula), height of the opercle vertically from the joint with the hyomandibula, lengths of the subopercle from the joint with the interopercle to the fork and to the posterior tip of the subopercle, and length of the interopercle from the anterior to posterior tips. We did not measure the preopercle, because it is functionally associated with the suspensorium rather than the operculum. Branchiostegal measurements were: lengths of the first six branchiostegal rays from their articulations with the ceratohyal to their posterior tip. Each species examined has six branchiostegal rays, except for *Dasycottus setiger* and *Artedius harringtoni*, which have seven. For size correction, we measured the length of the neurocranium from the anterior tip of the nasals to the posterior tip of the basioccipital, width of the neurocranium between the left and right joints of the neurocranium and hyomandibula, and maximum vertical height of the neurocranium. Although both the suspensorium and pectoral girdle are involved with suction feeding, we did not include them in our analyses due to substantial confounding factors, including the different developmental origins of the many suspensorial bones (Hulsey et al. 2005) and the role of the pectoral girdle in locomotion.

Testing hypotheses of evolutionary integration

To test for evolutionary correlation and covariation among the four mechanical units, we conducted the following analyses: (1) phylogenetic size correction of all measurements, (2) a phylogenetically corrected principal component analysis (pPCA) for each mechanical unit to reduce the dimensionality of the data, (3) correlations among phylogenetically independent contrasts computed from the first principle component axes (PC1) of each mechanical unit pPCA, and (4) tests of covariation among PC1 axes of each unit using phylogenetic generalized least squares (PGLS) models. We considered mechanical units to show evolutionary integration if both correlation of PIC contrasts and covariation of PC1 axes based on PGLS models were significant at $P = 0.05$. Analyses were conducted in R (R Core Team 2016) using the MCC tree from the best *MrBayes* run, as well as 500 trees randomly sampled from the posterior distribution of trees from this same *MrBayes* run (with 40% burn-in removed), with each tree successively used for all four analyses (Full code available on DataDryad, DOI:10.5061/dryad.gv3r544). We ultrametricized each tree using the *chronopl* function in the *ape* package (Paradis et al. 2004) and pruned each tree to include only the 45 taxa from our study using *drop.tip* in *ape* (Paradis et al. 2004). For size correction, we used the *phyl.resid* function in the *phytools* package (Revell 2009, 2012) to obtain residuals from PGLS regressions of each jaw, hyoid, opercular, and branchiostegal measurement against the geometric mean of head length, head width, and head height as a metric for head size. These residuals were used as phylogenetically size corrected data in our subsequent character analyses, as recommended by Revell (2009). For each of the four mechanical units, we reduced the dimensionality of measurements by performing a pPCA using the *phyl.pca* function in the *phytools* package (Revell 2009, 2012). We then extracted the PC1 axis. We used each PC1 to compute phylogenetically independent contrasts for each mechanical unit using the *pic* function in *ape* (Felsenstein 1985; Paradis et al. 2004). Correlations through the origin (Garland et al. 1992) were performed among contrasts of the four mechanical units, the jaws, hyoid, opercular bones, and branchiostegals, using the *cor.origin* function in the *PHYLOGR* package (Diaz-Uriarte and Garland 2014). Figure 3 summarizes these results, including biplots of PC1 PIC contrasts (lower left), and the distribution of correlation coefficients from each of the contrast pairs across 500 trees (upper right). To confirm that significant PIC correlations were associated with significant covariation between units, we tested for covariation using the *GLS* function in the *nlme* package (Pinheiro et al. 2018), with a Brownian Motion correlation structure computed from the phylogeny using the *corBrownian* function in *ape* (Paradis et al. 2004). The results of the PIC correlations and PGLS models are provided in Table 2 for both the MCC tree and for the posterior distribution of 500 trees from the best *MrBayes* run. We provide continuous character maps of the PC1 axis for each mechanical unit, made using the *contMap* function in phytools (Revell 2012), in Supplementary Fig. SA2.

To test whether we had sampled enough trees from the posterior distribution of trees from *MrBayes*, we randomly sampled 1–500 PGLS covariation coefficients from the above analysis of 500 trees and plotted mean coefficient against number of trees included. To test whether enough taxa were sampled, we resampled our pool of taxa 35 times to include a range of 10–45 species. We computed PGLS models

Table 2 Summary of statistical analyses

Mechanical Units	*r*	*P*	Covariance	*P*
Jaws vs. hyoid	−0.1846	0.2141	−0.2931	0.2246
Jaws vs. oper	0.3330*	0.0228	0.4080*	0.0254
Jaws vs. branch	0.5641*	3.633E−5	0.4568*	5.443E−5
Hyoid vs. oper	−0.2020	0.1733	−0.1559	0.1833
Hyoid vs. branch	−0.3983*	0.0056	−0.2032*	0.0067
Oper vs. branch	0.5142*	2.179E−4	0.3399*	3.023E−4
Jaws vs. hyoid	−0.2985 (±0.0089)	0.0975 (±0.0125)	−0.5377 (±0.0187)	0.1026 (±0.0127)
Jaws vs. oper	0.2964* (±0.0014)	0.0444 (±0.0013)	0.3819* (±0.0022)	0.0494 (±0.0013)
Jaws vs. branch	0.5637* (±0.0015)	4.841E−5 (±7.054E−6)	0.4854* (±0.0020)	7.037E−5 (±9.222E−6)
Hyoid vs. oper	−0.2212 (±0.0031)	0.1459 (±0.0062)	−0.1640 (±0.0031)	0.1548 (±0.0063)
Hyoid vs. branch	−0.4186* (±0.0022)	4.013E−3 (±2.559E−4)	−0.2058* (±0.0012)	4.891E−3 (±2.934E−4)
Oper vs. branch	0.5114* (±0.0021)	3.904E−4 (±5.072E−4)	0.3420* (±0.0018)	5.091E−4 (±1.347E−4)

Correlation coefficient for correlations of independent contrasts (*r*) and coefficients from PGLS models (covariance), with respective *P*-values. The top set of values is based on the MCC tree from the best *MrBayes* run. The bottom set of values are means based on a posterior distribution of 500 trees (after burnin) from the same *MrBayes* run, with 95% confidence intervals included in parentheses. Significant correlations are indicated with an asterisks.

across a distribution of 100 trees for each subsampled set of taxa and plotted the covariation coefficients against number of taxa included (Fig. 4).

Ecological analysis

To relate size of mechanical units to ecology, we used previously collected ecological data to conduct phylogenetically corrected ANOVAs on subsets of our taxa. We grouped 13 species of sculpins according to diet data from Norton (1995; Online Appendix Table SB2). Norton reported species diets by quantifying percent wet mass of each diet item within stomach contents of at least 16 individuals per species. We assigned each species a diet type, based on the prevalence of elusive, grasping, or easy prey in their diet. According to Norton, elusive prey can escape predation through locomotion, grasping prey cling to substrate, and easy prey can be captured with minimal resistance. We also assigned 21 species a habitat type (intertidal or subtidal), according to Eschmeyer et al. (1983). We also determined which species showed high levels of hypoxia tolerance using data for 11 species from Mandic et al. (2009, 2013). We tested for associations between diet, habitat, and hypoxia tolerance and each of the four mechanical units with phylogenetically corrected ANOVA models using the *GLS* function in the *nlme* package (Pinheiro et al. 2018), with a Brownian motion correlation structure computed from the phylogeny using *corBrownian* in *ape* (Paradis et al. 2004), along with the *anova* function (R Core Team 2016).

Results

Phylogenetic reconstruction

Based on the Shimodaira–Hasegawa test of 20 MCC trees, we identified one tree as the "best tree," with the topology that best explained our molecular data (Online Appendix Fig. SA1), and we used this tree and its posterior distribution of trees for all phylogenetic comparative methods. Four trees showed a significant difference from the best tree in the ability of their topologies to explain the molecular data. All trees recovered the Cottoidei clade (*sensu* Smith and Busby 2014) with high support, and 13 trees recovered Cottoidea (*sensu* Yabe 1985; Smith and Busby 2014; Online Appendix Table SA2). Our best tree (Online Appendix Fig. SA1) generally agrees with previous studies, particularly because we recovered a large monophyletic group of marine sculpins (Knope 2013 [unnamed clade]; Smith and Busby 2014 [Psychrolutidae]; Buser and López 2015 [unnamed clade]). However, our placement of the monotypic genera *Rhamphocottus*, *Jordania*, and *Leptocottus* within Cottoidea conflicts with previous studies (Knope 2013; Smith and Busby 2014). These problematic taxa are typically recovered at various positions among the non-psychrolutid cottoids with low node support (Knope 2013; Smith and Busby 2014), which is also the case in our analysis.

Character analyses

In the pPCA of mechanical units across the distribution of 500 trees, the PC1 axis explained 75.29–79.05% of the variance (77.78% median; 79.33%

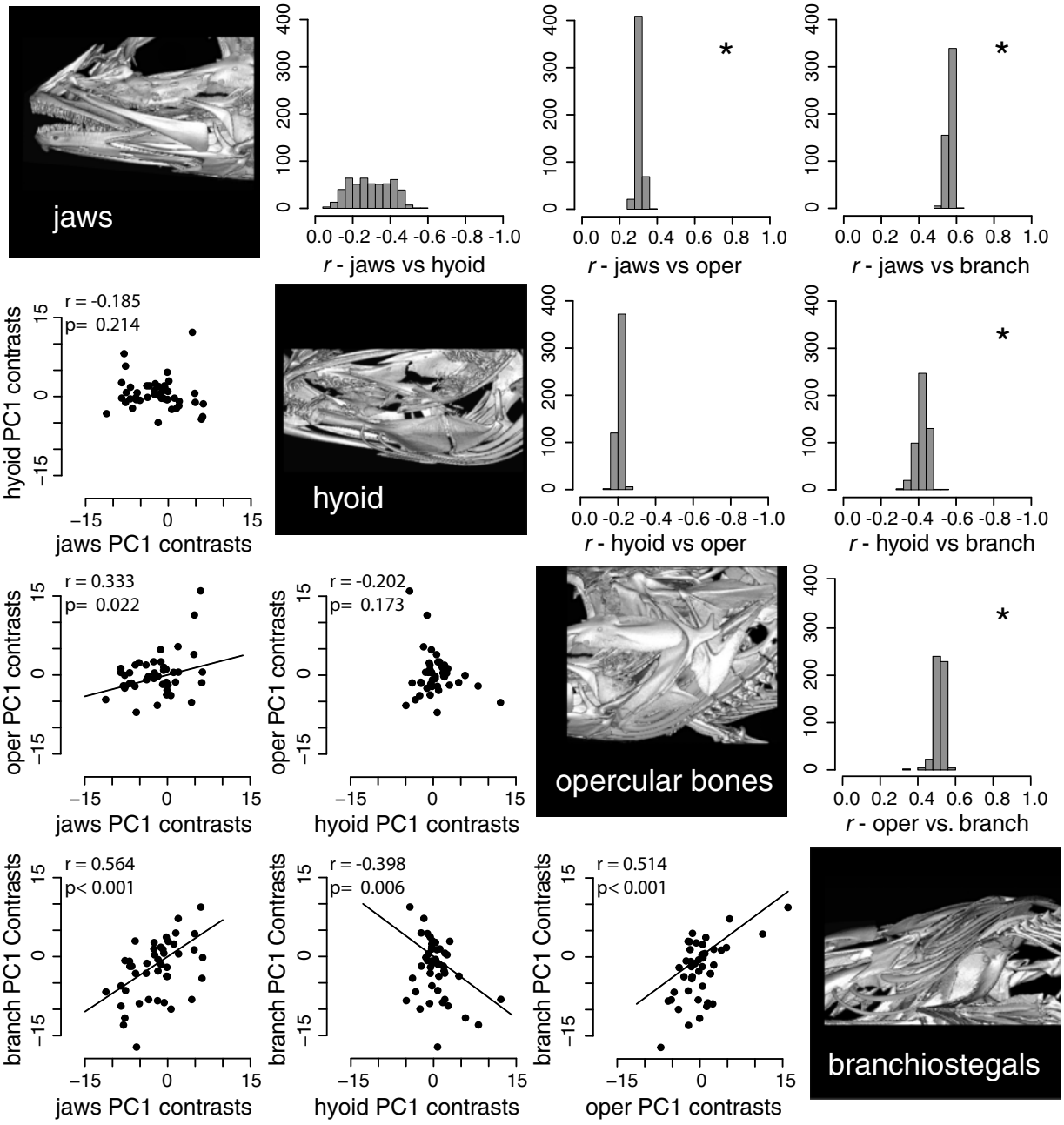

Fig. 3 Results of phylogenetically independent contrasts. The results of PIC correlations for each pair of mechanical units are shown in the lower left and upper right, with images of the structures from a micro-CT reconstruction in the center. We computed phylogenetically independent contrasts of PC1 scores from each mechanical unit pPCA to conduct correlations among our four mechanical units. Using the best MCC tree, we created bivariate plots of PC1 contrasts (lower left). Trendlines are shown for significant relationships. The distributions of correlation coefficients (*r*) across a posterior distribution of 500 trees are summarized by histograms (upper right). Among Cottoidei, we found significant positive evolutionary correlation among the jaws, opercular bones ("oper"), and branchiostegal rays ("branch"), with the hyoid showing no positive integration with any of the other mechanical units, and the hyoid was negatively correlated with the branchiostegal rays. Asterisks denote statistically significant correlations.

with MCC tree) for jaws and was mainly associated with variance in the dentary, anguloarticular length, maxilla, and premaxilla length. In pPCAs of hyoid measurements, PC1 explained 46.16–64.99% of the variance (50.70% median; 58.78% with MCC tree) and was mainly associated with variance in length of the anterior ceratohyal and the urohyal. In pPCAs of opercular bone measurements, PC1 explained 50.75–64.78% of the variance (55.92% median; 59.69% with MCC tree) and was mainly associated with variance in length of the subopercle from the joint with the interopercle to the posterior tip. In

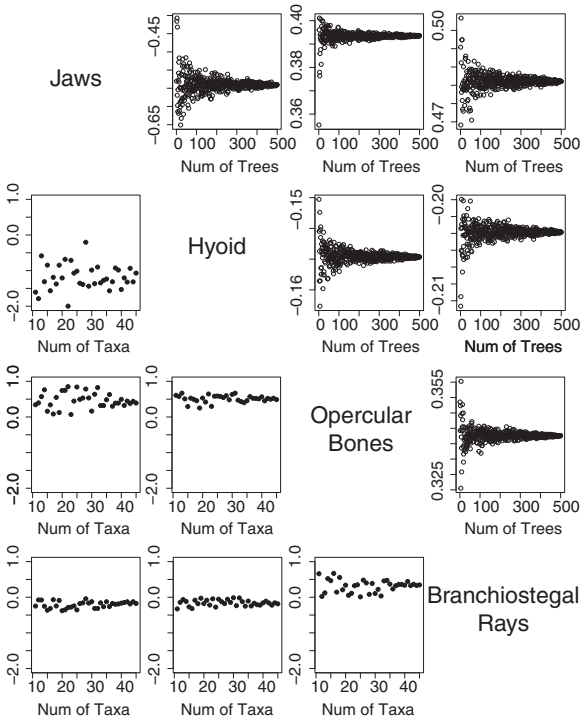

Fig. 4 Resampling analyses. To determine whether enough trees and taxa were sampled for consistent PGLS covariation coefficients, we randomly resampled PGLS covariation coefficients computed from 500 trees and plotted mean coefficient against number of trees included (top left), and we randomly resampled our pool of taxa to include 10–45 species and plotted mean coefficient against number of taxa included (bottom right). PGLS covariation coefficients became increasingly consistent with increasing number of taxa and trees, demonstrating that our sampling was sufficient. Each plot represents a regression between the mechanical unit labeled vertically and the unit labeled horizontally.

pPCAs of the branchiostegal measurements, PC1 explained 76.87–84.71% of the variance (82.44% median; 82.15% with MCC tree) and was loaded highly for all six branchiostegal ray lengths. Our plots of number of trees and number of taxa sampled against mean PGLS covariation coefficients showed a strong convergence toward the values reported in Table 2 (Fig. 4), and therefore, we concluded that we had sampled enough taxa and trees for this study.

PC1s of the pPCAs of the jaws, opercular bones, and branchiostegals were significantly positively evolutionarily correlated with one another ($P < 0.05$; Table 2). However, PC1 of the hyoid was not significantly positively correlated with any of the other mechanical units in any of the trees (Table 2 and Fig. 3). PC1 of the hyoid was significantly negatively correlated with PC1 of the branchiostegals ($P < 0.005$; Table 2). For phylogenetic ANOVAs with ecological traits (Fig. 5), sculpins that ate mainly elusive and grasping prey had larger jaws than species that ate easy prey ($P = 0.0131$), subtidal sculpins had larger hyoids than intertidal sculpins ($P = 0.0275$), and sculpins that were hypoxia tolerant had smaller hyoids than those with lower hypoxia tolerance ($P = 0.0074$). The opercular and branchiostegal mechanical units were not significantly associated with any of the ecological traits examined.

Discussion

Within Cottoidei, we found that the jaws, opercular bones, and branchiostegal rays show evolutionary integration (Table 1), as evidenced by significant evolutionary correlations among the PC1 axes of the pPCAs (Table 2 and Fig. 3). This is congruent with our third hypothesis based on the similar developmental origins of cranial dermal bone (dermal components of the jaws, opercular bones, and branchiostegal rays) relative to endochondral bone (hyoid). The coordinated evolution of mechanical units with similar development origins indicates that developmental pleiotropy within teleost skulls may produce developmental modularity on an evolutionary scale. Within Cottoidei, the independent evolution of the hyoid relative to other mechanical units of the skull may reduce limitations on morphological evolution of the suction feeding and gill ventilatory systems. Evolution of morphology within Cottoidei might otherwise be constrained by the high degree of functional coupling and functional coordination seen in teleost skulls (Hughes 1960; Lauder 1983, 1985; Collar et al. 2014). The relatively independent evolution of the hyoid in Cottoidei likely contributes to ecomorphological diversity of this clade.

Morphological integration and suction feeding

Suction feeding is widespread across teleost fishes, and the associated structures show substantial morphological diversity, despite the constraints of functional coordination, evolutionary integration, and coupling with other functions such as gill ventilation and occasionally parental care (Hoey et al. 2012; Tsuboi et al. 2015) or locomotion (Fish 1987; Pietsch and Grobecker 1987). Therefore, there must have existed sources of relaxed constraint on morphological evolution within the suction feeding system throughout the history of teleosts. The independent evolution of the hyoid relative to other mechanical units used for suction feeding is likely one of these mechanisms within Cottoidei. We speculate that independent evolution of the hyoid probably occurs within other clades of teleosts because the hyoid plays several key roles in suction feeding,

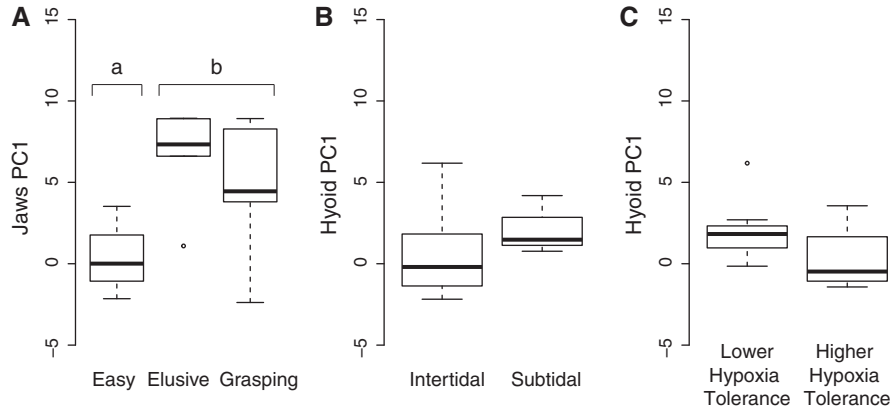

Fig. 5 Results of phylogenetic ANOVAs with ecological variables. We used data from studies of sculpin diet (Norton 1995), habitat (Eschmeyer et al. 1983), and hypoxia tolerance (Mandic et al. 2009, 2013) to fit phylogenetic ANOVA models to our four mechanical units. These boxplots represent the models that showed a significant relationship between ecology and morphology. Sculpins that eat elusive or grasping prey tend to have larger jaws (**A**; $P = 0.0131$), and sculpins that live in the intertidal zone (**B**; $P = 0.0275$) and those that are hypoxia tolerant (**C**; $P = 0.0074$) tend to have smaller hyoids.

and its relative size in different species likely is linked to its relative importance in fishes with different diets. For example, suction performance is thought to be maximized when peak suction corresponds with peak gape, which is made possible by hyoid depression that lags behind jaw depression (Gibb and Ferry-Graham 2005; Bishop et al. 2008; Wainwright et al. 2015), and therefore species with a larger hyoid can generate larger negative pressures during the peak-gape phase of suction. The hyoid is also critical to intraoral prey transport after the expansive phase of suction feeding, and often undergoes large excursions during prey processing and swallowing (Gillis and Lauder 1995).

In our analysis of cottoid diet data from Norton (1995), phylogenetic ANOVAs of 3 different prey types ("elusive prey," "grasping prey," and "easy prey") among 13 sculpin species (Fig. 5) showed that fishes that mostly eat grasping or elusive prey had larger jaws than those of fishes that eat easy prey (easy prey have "no major morphological defenses against capture once discovered;" Norton 1995: 64). This finding is consistent with Norton's conclusion that jaw size is largest in suction feeders that primarily eat elusive prey (Norton 1995). The increase in jaw size is likely due to a greater reliance on jaw protrusion to create a larger buccal volume change (Norton 1991, 1995; Carroll et al. 2004; Higham et al. 2007), increased hydrodynamic force (Holzman et al. 2008b; Wainwright and Longo 2017), and increased "jaw ram," in which jaw protrusion serves the additional purpose of bringing the opening of the mouth closer to the prey (Longo et al. 2016).

There is interest in evolutionary integration and functional coordination of body movements with suction feeding (Holzman et al. 2008a; Kane and Higham 2015; Longo et al. 2016), but studies that empirically test for integration among cranial units used in suction feeding are rare (Collar et al. 2014). Although we rejected our hypothesis of tight evolutionary integration among three major mechanical units of suction feeding (jaws, hyoid, and opercular bones: Fig. 2A), we demonstrated evolutionary integration of two mechanical units used in suction feeding (jaws and opercular bones). Opercular bones depress the lower jaw during the expansive phase of suction feeding. The opercle is extraordinarily diverse among teleosts, showing internal evolutionary and developmental modularity (Kimmel et al. 2017), and its correlated evolution with the jaws of sculpins may influence the diversity of suction feeding kinematics within this group. Together with the branchiostegal rays, the opercular bones also form the lateral wall of the gill chamber and contribute its expansion during suction feeding (Liem 1978). However, gill chamber expansion, facilitated by abduction of the opercular bones and lateral and ventral expansion of the branchiostegal apparatus, has almost no known influence on suction feeding pressures (Lauder 1980, 1983) and does not impact suction feeding performance other than potentially reducing backflow of water into the buccal chamber (Liem 1978). Therefore, although evolutionary correlation between jaw and opercular size may result from selection for suction feeding performance due to the linkage of opercular elements to lower jaw depression, it is unlikely that the correlation between

jaw and branchiostegal size plays a role in the evolution of suction feeding.

Morphological integration and gill ventilation

The branchiostegal rays and the membrane they support are a major source of diversity in gill ventilatory morphology (Baglioni 1907; Hughes 1960; McAllister 1968; Farina et al. 2015; Farina and Bemis 2016), and therefore it is surprising that they show such strong evolutionary correlation with other bones of the skull, especially the jaws. Based on gill ventilatory function, we hypothesized that the mechanical units of the buccal and gill chambers would show a high degree of evolutionary integration within chambers and little integration between chambers (H2; Fig. 2B). However, we did not find the expected integration between the jaws and hyoid as the primary mechanical units of the buccal chamber. The evolutionary integration between the mechanical units of the gill chamber (opercular bones and branchiostegals) may be due to the shared role of these structures in expanding and contracting the gill chamber during ventilation (Hughes 1960).

Major innovations within Cottoidei are related to their convergent invasion of the intertidal zone in multiple lineages (Ramon and Knope 2008; Buser et al. 2017). Oxygen availability is not as stable in the intertidal as in the subtidal, and therefore many intertidal sculpins have evolved hypoxia tolerance, air breathing, and the ability to walk between tide pools (Mandic et al. 2009, 2013; Bressman et al. 2018). In the subset of species analyzed, the hyoid was larger in subtidal sculpins and in species that had a low tolerance for hypoxia (Fig. 5). In benthic fishes such as cottoids, hyoid depression and elevation are the primary components of buccal expansion and compression (Hughes 1960). A large hyoid may provide a larger ventilatory stroke volume by producing a higher amplitude of buccal pumping. This would be efficient for subtidal fishes that can breathe slowly due to relatively stable oxygen availability, but intertidal fishes tend to reply on rapid rates of ventilation (Martin 1991) instead of high stroke volume. The negative evolutionary correlation between the hyoid and branchiostegal rays implies that sculpins with smaller hyoids tend to have larger branchiostegal rays, although branchiostegal size was not significantly predicted by hypoxia tolerance or tidal zone in our ecological analyses, suggesting that this negative evolutionary correlation is not indicative of an ecological trade-off.

Morphological integration and functional coupling

The overlap in mechanical units associated with suction feeding and gill ventilation in teleosts offers opportunities to examine co-evolving structures in coupled functions. Some suction-feeding vertebrates, including lungfishes and some elasmobranchs, decreased coupling between feeding and ventilatory structures through anatomical specializations of the suction feeding system (Bemis and Lauder 1986; Bemis 1987a, 1987b; Motta et al. 2002), yet teleost fishes have maintained an extremely close anatomical coupling between the two functions. Suction feeding is not simply an amplified gill ventilatory cycle, as evidenced by differences in the kinematics and pressure profiles observed during ventilation and suction feeding, including substantial differences in the relative magnitudes of pressures between the buccal and gill chambers (Hughes 1960; Liem 1970; Lauder 1980, 1983). Also, suction feeding often involves protrusion of the upper jaws and movement of some post-cranial elements, but these are less common in gill ventilation. Therefore, there are likely separate selective pressures shaping morphology and kinematics of these coupled functional systems. The relatively independent evolution of the hyoid may provide some of the evolutionary flexibility needed to respond to these selective pressures for both functions within Cottoidei and possibly within other teleost clades. This is supported by the association of the jaws and hyoid with different ecological characteristics (diet and hypoxia tolerance, respectively) related to both feeding and respiration. Differing developmental mechanisms acting upon endochondral and dermal bone also likely play a large role in the relatively independent evolution of the hyoid. Although it is difficult to directly link development to the evolution of function, it is likely that developmental modularity contributes to the evolutionary flexibility of this system (Albertson et al. 2003; Hulsey et al. 2005), allowing different units to respond independently to selection for different types of functional performance. We argue that investigations of the evolution of functional anatomical systems, particularly in vertebrates with complex musculoskeletal configurations, should simultaneously consider the constraining influence of functional coordination, evolutionary integration, and functional coupling whenever possible.

Acknowledgments

We would like to thank Drs. Amy McCune, Harry Greene, David Collar, Daniel Bolnick, Brian

Sidlauskas, Emily Kane, and anonymous reviewers for feedback during the development of this manuscript. We thank the faculty and students of Cornell University's ENTOM 4610 Model-Based Phylogenetics 2015 course, especially Dr. Elizabeth Murray. We also thank Drs. Liam Revell and Matthew Kolmann for statistical support. We thank Thaddaeus Buser for micro-CT scanning sculpins and making his scans publicly available. We thank the symposium speakers at the Society for Integrative Comparative Biology 2019 symposium "Multifunctional structures and multistructural functions: Functional coupling and integration in the evolution of biomechanical systems" for discussions on terminology and concepts that helped to further develop this manuscript.

Funding

This work was supported by the National Science Foundation [DEB-1310812 to S.C.F. and W.E.B.; DBI-1523836 to S.C.F.; DEB-1701665 to A.P.S.; and DBI-1759637 to A.P.S.]. Funding for the associated symposium was provided by SICB divisions DCB, DVM, DEDB, The Crustacean Society, American Microscopical Society as well as the National Science Foundation (IOS 1832822 to LP Hernandez).

Supplementary data

Supplementary data are available at *ICB* online.

References

Albertson RC, Streelman JT, Kocher TD. 2003. Directional selection has shaped the oral jaws of Lake Malawi cichlid fishes. Proc Natl Acad Sci U S A 100:5252–7.

Anker GC. 1974. Morphology and kinetics of the head of the stickleback, *Gasterosteus aculeatus*. Trans Zool Soc Lond 32:311–416.

Baglioni S. 1907. Der atmungsmechanismus der fische. Ein beitrag zur vergleichenden physiologie des atemrhythmus. Z Allg Physiol 7:177–282.

Bemis WE. 1987a. Feeding systems of living Dipnoi: anatomy and function. In: Bemis WE, Burggren WW, Kemp NE, editors. The biology and evolution of lungfishes. New York (NY): Alan Liss. p. 249–75.

Bemis WE. 1987b. Convergent evolution of jaw opening muscles in lungfishes and tetrapods. Can J Zool 65:2814–7.

Bemis WE, Lauder GV. 1986. Morphology and function of the feeding apparatus of the lungfish, *Lepidosiren paradoxa* (Dipnoi). J Morphol 187:81–108.

Benson DA, Cavanaugh M, Clark K, Karsch-Mizrachi I, Lipman DJ, Ostell J, Sayers EW. 2013. GenBank. Nucleic Acids Res 41:D36–42.

Bishop KL, Wainwright PC, Holzman R. 2008. Anterior-to-posterior wave of buccal expansion in suction feeding fishes is critical for optimizing fluid flow velocity profile. J R Soc Interface 5:1309–16.

Brainerd EL, Ferry-Graham LA. 2006. Mechanics of respiratory pumps. In: Shadwick RE, Lauder GV, editors. Fish physiology. Vol. 23. San Diego (CA): Elsevier Academic Press. p. 1–28.

Bressman NR, Gibb AC, Farina SC. 2018. A walking behavior generates functional overland movements in the tidepool sculpin, *Oligocottus maculosus*. Zoology 131:20–8.

Breuker CJ, Debat V, Klingenberg CP. 2006. Functional evo-devo. Trends Ecol Evol 21:488–92.

Buser TJ, Burns MD, López JA. 2017. Littorally adaptive? Testing the link between habitat, morphology, and reproduction in the intertidal sculpin subfamily Oligocottinae (Pisces: Cottoidea). PeerJ 5:e3634.

Buser TJ, López JA. 2015. Molecular phylogenetics of sculpins of the subfamily Oligocottinae (Cottidae). Mol Phylogenet Evol 86:64–74.

Camp AL, Brainerd EL. 2014. Role of axial muscles in powering mouth expansion during suction feeding in largemouth bass (*Micropterus salmoides*). J Exp Biol 217:1333–45.

Camp AL, Brainerd EL. 2015. Reevaluating musculoskeletal linkages in suction-feeding fishes with x-ray reconstruction of moving morphology (XROMM). Integr Comp Biol 55:36–47.

Carroll AM, Wainwright PC, Huskey SH, Collar DC, Turingan RG. 2004. Morphology predicts suction feeding performance in centrarchid fishes. J Exp Biol 207:3873–81.

Cheverud JM. 1982. Phenotypic, genetic, and environmental morphological integration in the cranium. Evolution 36:499–516.

Cheverud JM. 1996. Developmental integration and the evolution of pleiotropy. Am Zool 36:44–50.

Claverie T, Patek SN. 2013. Modularity and rates of evolutionary change in a power-amplified prey capture system. Evolution 67:3191–207.

Córdoba SA, Cocucci AA. 2011. Flower power: its association with bee power and floral functional morphology in papilionate legumes. Ann Bot 108:919–31.

Collar DC, Wainwright PC, Alfaro ME, Revell LJ, Mehta RS. 2014. A novel feeding mode disrupts evolutionary integration of the skull in eels. Nat Commun 5:5505.

Darriba D, Taboada GL, Doallo R, Posada D. 2012. jModelTest 2: more models, new heuristics and parallel computing. Nat Methods 9:772.

de Beer GR. 1937. Development of the vertebrate skull. Oxford: Oxford University Press.

Diaz-Uriarte R, Garland T. 2014. PHYLOGR: functions for phylogenetically based statistical analyses. R package version 1.0.8 (http://CRAN.R-project.org/package=PHYLOGR).

Dudley R. 2002. The biomechanics of insect flight: form, function, evolution. Princeton (NJ): Princeton University Press.

Edgar RC. 2004. MUSCLE: multiple sequence alignment with high accuracy and high throughput. Nucleic Acids Res 32:1792–7.

Eschmeyer WN, Fong JD. 2009. Species by family/subfamily. (http://researcharchive.calacademy.org/research/ichthyology/catalog/SpeciesByFamily.asp; accessed 20 January 2019).

Eschmeyer WN, Herald ES, Hammann H. 1983. A field guide to Pacific coast fishes of North America.Boston (MA): Houghton Mifflin Co.

Farina SC, Bemis WE. 2016. Functional morphology of gill ventilation of the goosefish, *Lophius americanus* (Lophiiformes: Lophiidae). Zoology 119:207–15.
Farina SC, Near TJ, Bemis WE. 2015. Evolution of the branchiostegal membrane and restricted gill openings in Actinopterygian fishes. J Morphol 276:681–94.
Felice RN, Randau M, Goswami A. 2018. A fly in a tube: Macroevolutionary expectations for integrated phenotypes. Evolution 72:2580–94.
Felsenstein J. 1981. Evolutionary trees from DNA sequences: a maximum likelihood approach. J Mol Evol 17:368–76.
Felsenstein J. 1985. Phylogenies and the comparative method. Am Nat 125:1–15.
Fish FE. 1987. Kinematics and power output of jet propulsion by the frogfish genus *Antennarius* (Lophiiformes: Antennariidae). Copeia 1987:1046–8.
Garland T, Harvey PH, Ives AR. 1992. Procedures for the analysis of comparative data using phylogenetically independent contrasts. Syst Biol 41:18–32.
Gibb AC, Ferry-Graham LA. 2005. Cranial movements during suction feeding in teleost fishes: are they modified to enhance suction production? Zoology 108:141–53.
Gillis G, Lauder GV. 1995. Kinematics of feeding in bluegill sunfish: is there a general distinction between aquatic capture and transport behaviors? J Exp Biol 198:709–20.
Glubokov AI, Orlov AM. 2008. Data on distribution and biology of poachers Agonidae from the northwestern part of the Bering Sea. J Ichthyol 48:426–42.
Goswami A. 2006. Cranial modularity shifts during mammalian evolution. Am Nat 168:270–80.
Goswami A, Polly PD. 2010. The influence of modularity on cranial morphological disparity in Carnivora and primates (Mammalia). PLoS ONE 5:e9517.
Goswami A, Smaers JB, Soligo C, Polly PD. 2014. The macroevolutionary consequences of phenotypic integration: from development to deep time. Philos Trans R Soc B 369:20130254.
Grande L, Bemis WE. 1998. A comprehensive phylogenetic study of amiid fishes (Amiidae) based on comparative skeletal anatomy. An empirical search for interconnected patterns of natural history. J Vertebr Paleontol 18:1–696 (special memoir #4 1–690 + ix).
Guindon S, Gascuel O. 2003. A simple, fast and accurate method to estimate large phylogenies by maximum-likelihood. Syst Biol 52:696–704.
Hall BK. 2015. Bones and cartilage. Developmental and evolutionary skeletal biology. 2nd ed. San Diego, CA: Academic Press.
Higham TE, Hulsey CD, Rícan O, Carroll AM. 2007. Feeding with speed: prey capture evolution in cichlids. J Evol Biol 20:70–8.
Hoey AS, Bellwood DR, Barnett A. 2012. To feed or to breed: morphological constraints of mouthbrooding in coral reef cardinalfishes. Proc R Soc Lond [Biol] 279:2426–32.
Holzman R, Day SW, Mehta RS, Wainwright PC. 2008. Integrating the determinants of suction feeding performance in centrarchid fishes. J Exp Biol 211:3296–305.
Holzman R, Day SW, Mehta RS, Wainwright PC. 2008. Jaw protrusion enhances forces exerted on prey by suction feeding fishes. J R Soc Interface 5:1445–57.
Hughes GM. 1960. A comparative study of gill ventilation in marine teleosts. J Exp Biol 37:28–45.
Hughes GM, Shelton G. 1958. The mechanism of gill ventilation in three freshwater teleosts. J Exp Biol 35:807–23.
Hulsey CD, Fraser GJ, Streelman JT. 2005. Evolution and development of complex biomechanical systems: 300 million years of fish jaws. Zebrafish 2:243–57.
Johansson LC, Engel S, Baird E, Dacke M, Muijres FT, Hedenstrom A. 2012. Elytra boost lift, but reduce aerodynamic efficiency in flying beetles. J R Soc Interface 9:2745–8.
Kane EA, Higham TE. 2015. Complex systems are more than the sum of their parts: using integration to understand performance, biomechanics, and diversity. Integr Comp Biol 55:146–65.
Kaufman LS, Liem KF. 1982. Fishes of the suborder Labroidei (Pisces: Perciformes): phylogeny, ecology, and evolutionary significance. Breviora 472:1–19.
Kimmel CB, Small CM, Knope ML. 2017. A rich diversity of opercle bone shape among teleost fishes. PLoS ONE 12:e0188888.
Klingenberg CP. 2008. Morphological integration and developmental modularity. Annu Rev Ecol Evol Syst 39:115–32.
Klingenberg CP, Marugán-Lobón J. 2013. Evolutionary covariation in geometric morphometric data: analyzing integration, modularity, and allometry in a phylogenetic context. Syst Biol 62:591–610.
Knope ML. 2013. Phylogenetics of the marine sculpins (Teleostei: Cottidae) of the North American Pacific Coast. Mol Phylogenet Evol 66:341–9.
Knope ML, Scales JA. 2013. Adaptive morphological shifts to novel habitats in marine sculpin fishes. J Evol Biol 26:472–82.
Lauder GV. 1980. The suction feeding mechanism in sunfishes (*Lepomis*): an experimental analysis. J Exp Biol 88:49–72.
Lauder GV. 1981. Form and function: structural analysis in evolutionary morphology. Paleobiology 7:430–42.
Lauder GV. 1982. Patterns of evolution in the feeding mechanism of actinopterygian fishes. Am Zool 22:275–85.
Lauder GV. 1983. Prey capture hydrodynamics in fishes: experimental tests of two models. J Exp Biol 104:1–13.
Lauder GV. 1985. Aquatic feeding in lower vertebrates. In: Hildebrand M, Bramble DM, Liem KF, Wake DB, editors. Functional vertebrate morphology. Cambridge: Harvard University Press. p. 210–29.
Lawrence JF, Ślipiński A, Seago AE, Thayer MK, Newton AF, Marvaldi AE. 2011. Phylogeny of the Coleoptera based on morphological characters of adults and larvae. Ann Zool 61:1–218.
Li W, Cowley A, Uludag M, Gur T, McWilliam H, Squizzato S, Park YM, Buso N, Lopez R. 2015. The EMBL-EBI bioinformatics and programmatic tools framework. Nucleic Acids Res 43:W580–4.
Liem KF. 1970. Comparative functional anatomy of the Nandidae (Pisces: Teleostei). Fieldiana Zool 56:1–166.
Liem KF. 1973. Evolutionary strategies and morphological innovations: cichlid pharyngeal jaws. Syst Zool 22:425–41.

Liem KF. 1978. Modularity multiplicity in the functional repertoire of the feeding mechanism in cichlid fishes. I. Piscivores. J Morphol 158:323–60.

Longo SJ, McGee MD, Oufiero CE, Waltzek TB, Wainwright PC. 2016. Body ram, not suction, is the primary axis of suction-feeding diversity in spiny-rayed fishes. J Exp Biol 219:119–28.

Mandic M, Speers-Roesch B, Richards JG. 2013. Hypoxia tolerance in sculpins is associated with high anaerobic enzyme activity in brain but not in liver or muscle. Physiol Biochem Zool 86:92–105.

Mandic M, Todgham AE, Richards JG. 2009. Mechanisms and evolution of hypoxia tolerance in fish. Proc R Soc Lond [Biol] 276:735–44.

Martin KLM. 1991. Facultative aerial respiration in an intertidal sculpin, *Clinocottus analis* (Scorpaeniformes: Cottidae). Physiol Biochem 64:1341–55.

McAllister DE. 1968. Evolution of branchiostegals and classification of teleostome fishes. Bull Natl Mus Canada 221:1–237.

Monteiro LR, Nogueira MR. 2010. Adaptive radiations, ecological specialization, and the evolutionary integration of complex morphological structures. Evolution 64:724–44.

Motta PJ, Hueter RE, Tricas TC, Summers AP. 2002. Kinematic analysis of suction feeding in the nurse shark, *Ginglymostoma cirratum* (Orectolobiformes, Ginglymostomatidae). Copeia 2002:24–38.

Napazakov VV, Chuchukalo VI. 2005. Feeding of liparids (Liparidae) in the western Bering Sea. J Ichthyol 45:313–7.

Norton SF. 1991. Capture success and diet of cottid fishes: the role of predator morphology and attack kinematics. Ecology 72:1807–19.

Norton SF. 1995. A functional approach to ecomorphological patterns of feeding in cottid fishes. Environ Biol Fish 44:61–78.

Olson EC, Miller RL. 1958. Morphological integration. Chicago, IL: University of Chicago Press.

Paradis E, Claude J, Strimmer K. 2004. APE: analyses of phylogenetics and evolution in R language. Bioinformatics 20:289–90.

Parnell NF, Hulsey CD, Streelman JT. 2012. The genetic basis of a complex functional system. Evolution 66:3352–66.

Parsons KJ, Son YH, Crespel A, Thambithurai D, Killen S, Harris MP, Albertson RC. 2018. Conserved but flexible modularity in the zebrafish skull: implications for craniofacial evolvability. Proc R Soc B Biol Sci 285:20172671.

Parsons KJ, Son YH, Albertson RC. 2011. Hybridization promotes evolvability in African cichlids: connections between transgressive segregation and phenotypic integration. Evol Biol 38:306–15.

Pietsch TW, Grobecker DB. 1987. Frogfishes of the world. Stanford (CA): Stanford University Press.

Pinheiro J, Bates D, DebRoy S, Sarkar D; R Core Team. 2018. *nlme*: linear and nonlinear mixed effects models. R package version 3.1-137 (https://CRAN.R-project.org/package=nlme).

R Core Team. 2016. R: a language and environment for statistical computing. Vienna, Austria: R Foundation for Statistical Computing (https://www.R-project.org).

Rambaut A, Suchard MS, Xie D, Drummond AJ. 2014. Tracer v1.6 (http://beast.bio.ed.ac.uk/Tracer).

Ramon ML, Knope ML. 2008. Molecular support for marine sculpin (Cottidae; Oligocottinae) diversification during the transition from the subtidal to intertidal habitat in the Northeastern Pacific Ocean. Mol Phylogenet Evol 46:475–83.

Revell LJ. 2009. Size-correction and principal components for interspecific comparative studies. Evolution 63:3258–68.

Revell LJ. 2012. phytools: an R package for phylogenetic comparative biology (and other things). Methods Ecol Evol 3:217–23.

Roberts AS, Farina SC, Goforth RR, Gidmark NJ. 2018. Evolution of skeletal and muscular morphology within the functionally integrated lower jaw adduction system of sculpins and relatives (Cottoidei). Zoology 129:59–65.

Ronquist F, Teslenko M, van der Mark P, Ayres DL, Darling A, Höhna S, Larget B, Liu L, Suchard MA, Huelsenbeck JP. 2012. MrBayes 3.2: efficient Bayesian phylogenetic inference and model choice across a large model space. Syst Biol 61:539–42.

Rosset A, Spadola L, Ratib O. 2004. OsiriX: an open-source software for navigating in multidimensional DICOM images. J Digital Imaging 17:205–16.

Sanford CPJ, Wainwright PC. 2002. Use of sonomicrometry demonstrates the link between prey capture kinematics and suction pressures in Largemouth Bass. J Exp Biol 205:3445–57.

Schaefer SA, Lauder GV. 1996. Testing historical hypotheses of morphological change: biomechanical decoupling in loricarioid catfishes. Evolution 50:1661–75.

Schliep KP. 2011. phangorn: phylogenetic analysis in R. Bioinformatics 27:592–3.

Schwenk K, Wagner GP. 2001. Function and the evolution of phenotypic stability: connecting pattern to process. Am Zool 41:552–63.

Shimodaira H, Hasegawa M. 1999. Multiple comparisons of log-likelihoods with applications to phylogenetic inference. Mol Biol Evol 16:1114–6.

Smith WL, Busby MS. 2014. Phylogeny and taxonomy of sculpins, sandfishes, and snailfishes (Perciformes: Cottoidei) with comments on the phylogenetic significance of their early-life-history specializations. Mol Phylogenet Evol 79:332–52.

Smith WL, Wheeler WC. 2004. Polyphyly of the mail-cheeked fishes (Teleostei: Scorpaeniformes): evidence from mitochondrial and nuclear sequence data. Mol Phylogenet Evol 32:627–46.

Tavaré S. 1986. Some probabilistic and statistical problems in the analysis of DNA sequences. Lect Math Life Sci 17:57–86.

Thedinga JF, Johnson SW, Mortensen DG. 2006. Habitat, age, and diet of a forage fish in southeastern Alaska: Pacific sandfish (*Trichodon trichodon*). Fish Bull 104:631–7.

Tsuboi M, Gonzalez-Voyer A, Kolm N. 2015. Functional coupling constrains craniofacial diversification in Lake Tanganyika cichlids. Biol Lett 11:20141053.

van der Laan R, Eschmeyer WN, Fricke R. 2014. Family-group names of recent fishes. Zootaxa 3882:1–230.

Wainwright PC. 2006. Functional morphology of the pharyngeal jaw apparatus. In: Shadwick RE, Lauder GV, editors.

Fish physiology. Vol. 23. San Diego (CA): Elsevier Academic Press. p. 79–101.
Wainwright PC. 2007. Functional versus morphological diversity in macroevolution. Annu Rev Ecol Evol Syst 38:381–401.
Wainwright PC, Longo SJ. 2017. Functional innovations and the conquest of the oceans by acanthomorph fishes. Curr Biol 27:R550–7.
Wainwright PC, McGee MD, Longo SJ, Hernandez LP. 2015. Origins, innovations, and diversification of suction feeding in vertebrates. Integr Comp Biol 55:134–45.
Walker JA. 2010. An integrative model of evolutionary covariance: a symposium on body shape in fishes. Integr Comp Biol 50:1051–6.
Yabe M. 1985. Comparative osteology and myology of the superfamily Cottoidea (Pisces: Scorpaeniformes) and its phylogenetic classification. Memoirs of the Faculty of Fisheries-Hokkaido University, Japan.
Young NM, Hallgrímsson B. 2005. Serial homology and the evolution of mammalian limb covariation structure. Evolution 59:2691–704.